Assessing parameter uncertainty in semi-distributed hydrological model based on type-2 fuzzy analysis: a case study of Kaidu River Basin

C. X. Wang, Y. P. Li, J. L. Zhang and G. H. Huang

ABSTRACT

In this study, a type-2 fuzzy simulation method (TFSM) is developed for modeling hydrological processes associated with vague information through coupling type-2 fuzzy analysis technique with the semi-distributed land use based runoff processes (SLURP) model. TFSM can handle fuzzy sets with uncertain membership function related to hydrological modeling parameters and reveal the effects of such uncertain parameters on the hydrological processes. Streamflow calibration and verification are performed using the hydrological data for the Kaidu River Basin, China. The statistical values of Nash–Sutcliffe efficiency, determination coefficient, and deviation of volume indicate a good performance of SLURP in describing the streamflow at the outlet of the Kaidu River Basin. Based on TFSM, the effects of four uncertain parameters such as precipitation factor (PF), maximum capacity for fast store, retention constant for fast store (RF), and retention constant for slow store, on the hydrological processes are analyzed under different α-cut levels. Results demonstrate that the uncertainty associated with PF has significant effect on the simulated streamflow, while the uncertainty associated with RF has slight effect among the four parameters. These findings are helpful for improving efficiency in hydrological prediction and enhancing the model applicability.

Key words | hydrological simulation, Kaidu River Basin, streamflow, type-2 fuzzy sets, uncertainty analysis

C. X. Wang
Y. P. Li (corresponding author)
J. L. Zhang
G. H. Huang
MOE Key Laboratory of Regional Energy Systems Optimization,
Sino-Canada Resources and Environmental Research Academy,
North China Electric Power University,
Beijing 102206,
China
E-mail: *yongping.li@iseis.org*

INTRODUCTION

Investigating the dynamic characteristic of hydrological processes as well as the detailed information on streamflow response is of vital significance for conserving and restoring the eco-environment in arid and semi-arid regions. Hydrological models are important tools for providing catchment management with information on the interaction of water, energy, and vegetation processes distributed over space and time in a way that cannot be conducted through field experiment and direct observation (Benke *et al.* 2008). Owing to the increasing availabilities of digital elevation models (DEMs), geographical information system, remote sensing, and terrain analysis tools over a broad range of scales, many hydrological models have been widely used for analyzing water balance, forecasting long-range streamflow, predicting real-time flood, and investigating climate-change impact in watershed management and planning (Lenhart *et al.* 2003; Ahn *et al.* 2010; Vincendon *et al.* 2010; Bastola & Murphy 2013; Kizza *et al.* 2013; O'Loughlin *et al.* 2013; Hughes *et al.* 2014; Wang *et al.* 2014; Westerberg *et al.* 2014; Shiri *et al.* 2015). For example, Lenhart *et al.* (2003) modified the soil and water assessment tool (SWAT) model for improving flow prediction (e.g. percolation, hydraulic conductivity, and interflow) of low mountain areas in Germany. Ahn *et al.* (2010) assessed the impact of land use changes on streamflow and groundwater recharge through considering future potential climate and land use changes using the semi-distributed land use based runoff processes (SLURP) model. Vincendon *et al.* (2010)

doi: 10.2166/nh.2015.226

integrated soil, biosphere, and atmosphere land surface model and topography based rainfall–runoff model to simulate Mediterranean flash floods, demonstrating a good ability for flood forecasting. These models can effectively investigate the watershed hydrological responses. However, in many real-world problems, model representations of real-world hydrological systems are complicated with a variety of factors, such as inadequate conceptualizations of physical processes, errors related to spatial and temporal scales of model and derivation of model parameter values directly from basin traits (Guerrero *et al.* 2013). In addition, parameters obtained from calibration are also affected by several factors such as correlations among parameters, sensitivity or insensitivity in parameters, and statistical features of model residuals. Neglecting these uncertainties can result in increased risk of failures in hydrological forecasting and related infrastructure design, suggesting an urgent need to assess the parameter uncertainty involved in hydrological simulations.

Consequently, a number of efforts were undertaken in developing more effective methods for reflecting parameter uncertainty in hydrological models and their effects on modeling performances (Muleta & Nicklow 2005; Arabi *et al.* 2007; Zhang *et al.* 2009; Jeremiah *et al.* 2012; Hughes *et al.* 2013; Li *et al.* 2013; Mahiny & Clarke 2013; Zhou *et al.* 2013; Bourgault *et al.* 2014; Ling *et al.* 2014; Ma *et al.* 2014; Charles & Parick 2015; Patel & Rahman 2015). For example, Muleta & Nicklow (2005) incorporated a generalized likelihood uncertainty estimation method within SWAT for calibrating daily streamflow and daily sediment concentration values in the Big Creek watershed, where uncertainties of model parameters were investigated and streamflow and sediment yield estimation were both improved. Arabi *et al.* (2007) integrated Monte Carlo-based simulation method into SWAT to analyze the uncertainty in model estimates of water quality benefits in the Black Creek watershed; the method could adjust the suggested range of model parameters to more realistic site-specific ranges based on observed data. Zhang *et al.* (2009) presented a genetic algorithm and Bayesian method to analyze parameter uncertainty of SWAT; uncertainty intervals were estimated in the little river experimental basin in Georgia and the Headwater area of Yellow River. Li *et al.* (2013) employed the bootstrap method to estimate parameter uncertainty in a lumped conceptual water balance model; the results demonstrated that simulation uncertainties caused by co-effects of model parameters and model structure could be evaluated effectively. Charles & Parick (2015) assessed the uncertainty in the calibration of the generalized Pareto distribution to rainfall extremes based on observation in the Lake Victoria Basin, where the Jackknife technique and non-parametric percentile bootstrapping method were combined to quantify uncertainty in the extreme intensity quantifies. In general, although the stochastic analysis method is capable of handling uncertainties with known probability distributions, several limitations still remain, including the following: (i) it requires subjective decisions on the likelihood function and has massive computing resources for high dimensional parameter space; and (ii) it cannot ensure a sufficient precision of the statistics inferred from the retained solutions unless the sampling of the parameter space is dense enough (Blasone *et al.* 2008).

The fuzzy analysis technique is useful for dealing with vagueness and ambiguity based on fuzzy sets theory, where uncertainties are handled in a direct way without a large number of realizations (Li & Huang 2009). The conventional fuzzy analysis techniques can solve the problems containing fuzzy sets (e.g. (b_1, b_0, b_2) with triangular membership function or (b_1, b_2, b_3, b_4) with trapezoidal membership function), whose membership grade (e.g. $u(x)$) is a real number in [0, 1]. In fact, the membership grade can be uncertain (i.e. cannot be expressed as precision information) due to change of natural condition, limitation of weather monitoring, and lack of hydrological data. For example, in hydrological models, the soil infiltration rate involves a number of processes and factors, such as seepage pattern, soil type and geologic feature; the temporal and spatial distribution characteristics of these processes and factors further lead to complex infiltration processes that vary from one location to another and can result in uncertainties in hydrological modeling. Such uncertainties may be further multiplied by the sampling error because of spatial non-uniformity of the precipitation and the small number of sampling. As a result, these parameters may be estimated as fuzzy sets with inexact membership function, leading to type-2 fuzzy sets $(\tilde{k}^l, k_0, \tilde{k}^u)$ (abbreviated as T2FS), whose left- and right-end points ($\tilde{k}^l$ and $\tilde{k}^u$) are

uncertain. Nevertheless, previous fuzzy analysis approaches had difficulties in tacking such T2FS in hydrological models.

The Tarim River Basin is a typical arid region, which is characterized by low and irregular rainfall, high temperature and evaporation, and notable drought periods (Huang *et al.* 2010). Kaidu River is one of the main tributaries that discharge into the Tarim River. It plays an important role in protecting biodiversity, reducing the impact of sandstorms, moderating desertification, regulating oasis climate, and maintaining ecosystem balance of the green corridor of the lower reaches of the Tarim River. Massive exploitation and construction have made the regional water resources system degrade and brought about severe damage to the local ecological and environmental sustainability. For instance, massive water extraction for agricultural irrigation along the river course has seriously decreased the natural vegetation and natural streamflow, and subsequently results in the desiccation for the lower reaches and the terminal lakes, salinization for soils and waters, vegetation degradation for floodplain (Aishan *et al.* 2013). On the other hand, the landscape is sparsely populated, with large areas being remote and inaccessible; regular monitoring is difficult and large investment is required. Furthermore, precise data are difficult to obtain due to temporal and spatial variations in hydrological processes. These may be further compounded by uncertainties inherently existing in system components concerned with precipitation, topography, and evapotranspiration, creating complexities which are beyond the traditional hydrological simulation techniques.

Therefore, this study aims to develop a type-2 fuzzy simulation method (TFSM) for modeling hydrological processes of the Kaidu River Basin associated with vague information, through coupling type-2 fuzzy analysis technique with the SLURP model. The SLURP model is used for dealing with spatial and temporal variations of hydrological elements and accounting for physical mechanisms of runoff yield and routing in the study basin. Type-2 fuzzy analysis technique specializes in facilitating the characterization of hydrogeological parameters and sampling from uncertain possibility distributions based on α-cut levels for sensitivity analysis. The results will help to quantify the effects of parameter uncertainties on hydrological simulations. The parameter with the most significant effect on the modeling performance can also be disclosed.

METHODOLOGY

SLURP model

The SLURP model is a continuous-time, distributed-parameter, physically based model. The model initially divides a basin into multiple aggregated simulation areas (ASAs), which are then further subdivided into their component land covers using the topographic parameterization package (TOPAZ). The vertical water balance concept applied to each land type within an ASA is four non-linear tanks, i.e. canopy storage, snow storage, fast storage and slow storage, representing canopy interception, snowpack, aerated soil storage, and groundwater, respectively (Han *et al.* 2014). In SLURP, the Granger method is used to calculate evapotranspiration E (mm) for each land cover

$$E = \frac{\Delta G + \gamma G E_a}{\Delta G + \gamma} \tag{1}$$

$$G = \frac{1}{0.905 + 0.095e^{(6.2D)}} + 0.2(1 - D) \tag{2}$$

$$D = \frac{f_u(e_a^* - e_a)}{f_u(e_a^* - e_a) + Q_N} \tag{3}$$

where Δ is the slope of the vapor pressure curve (kPa/°C), G is the relative evaporation (dimensionless), Q_N is the net radiation (mm eq./d), γ is the psychometric constant (0.066 kPa/°C), f_u is the wind speed function (mm/d kPa), e the vapor pressure (kPa), and e_a^* is the saturated vapor pressure at the air temperature (kPa). Snowmelt is calculated using the degree-day method. Rainfall and any snowmelt infiltrates through soil surface into the fast store depending on the current infiltration rate. If precipitation intensity exceeds the maximum possible infiltration rate, surface runoff is generated using the following equations:

$$\ln f = \left(1 - \frac{S_1}{S_{1,\max}}\right) \cdot \ln f_{\max} \tag{4}$$

$$Q_s = (p - \ln f) \cdot t \tag{5}$$

where p is the precipitation intensity, t is the delay of rainfall, S_1 is the current contents of the fast store, $S_{1,\max}$ is the maximum capacity of the fast store and $\ln f_{\max}$ is the maximum possible infiltration rate. The subsurface flow processes are simulated using two linear reservoirs, the fast store, which may be considered as an unsaturated soil layer contributing surface runoff, and the slow store, which may be considered as a groundwater zone. Generally, the simulation of subsurface flow processes is based on the following equations:

$$\mathrm{RP} + \mathrm{RI} = \frac{1}{k_1} \cdot S_1 \tag{6}$$

$$\frac{\mathrm{RP}}{\mathrm{RI}} = \frac{S_1/S_{1,\max}}{S_2/S_{2,\max}} \tag{7}$$

$$\mathrm{RG} = \frac{1}{k_2} \cdot S_2 \tag{8}$$

where RP is the amount of percolation, RI is the amount of interflow, RG is the amount of groundwater flow, k_1 is the retention constant for fast store (RF), k_2 is the retention constant for slow store (RS), S_2 is the current contents for slow store, and $S_{2,\max}$ is the maximum contents of the slow store.

Generally, SLURP can incorporate the necessary physics while retaining comparative simplicity of operation; it has a physical mechanism which simulates hydrological cycle from precipitation to runoff, including the effects of water extractions and irrigation schemes. In hydrological modeling processes, when intensive data collection is possible, model parameters are measured or estimated from watershed characteristics. Owing to the unknown spatial heterogeneity of parameter values as well as the high cost involved in field experiments or measurements, some parameters can only be determined by calibrating the model against the observations of watershed export. However, hydrological simulation is significantly influenced by uncertainties from sources other than the obtained daily hydrological data. The major sources contributing to the hydrological uncertainty include parametric and structural uncertainties in the hydrological models and uncertainty in the model initial conditions. These uncertainties can further lead to imprecise/vague modeling parameters. Therefore, it is essential that the water movement is simulated under parameter uncertainties in order to provide robust information for hydrological forecasting and related infrastructure design.

Type-2 fuzzy analysis technique

T2FS, as extensions of conventional fuzzy sets, are defined as sets whose membership function is also fuzzy, i.e. the membership grade of each element is no longer a crisp value but a fuzzy set. The general notation of a T2FS can be presented as follows (Aliev *et al.* 2011):

$$\tilde{\tilde{A}}(x) = \{((x, u), \tilde{u}_{\tilde{A}}(x, u)) : \forall x \in X,\ \forall u \in J_x\} \tag{9}$$

where x is the primary variable in domain X; u is the secondary variable in domain J_x; $J_x \subseteq [0, 1]$ is the primary membership; $\tilde{u}_{\tilde{A}}(x, u) \subseteq [0, 1]$ is the secondary membership function or type-2 membership function, as shown in Figure 1. A T2FS can be characterized by the footprint of uncertainty (FOU) which is bound by a lower membership function $\tilde{A}^l(x)$ (LMF), and an upper membership function $\tilde{A}^u(x)$ (UMF). Therefore, the FOU of T2FS can be defined as follows:

$$\mathrm{FOU}(\tilde{A}) = \bigcup_{x \in X} [\tilde{A}^l(x), \tilde{A}^u(x)] \tag{10}$$

Type-2 fuzzy analysis technique is a class of algorithms for sampling from uncertain possibility distributions based on α-cut levels (i.e. dividing input membership domain into a series of equally spaced α-cut levels). For each α-cut, the lower and upper bounds as well as their interior points of each fuzzy variable are selected. With different combinations of these points being used as input values, parameter uncertainty can be tackled by modeling results. The T2FS ($\tilde{\tilde{A}}$) with α-cut level can be expressed as

$$\tilde{A}_\alpha = \{x \in X | \mu_{\tilde{A}^l}(x) \geq \alpha, \mu_{\tilde{A}^u}(x) \geq \alpha\} \tag{11}$$

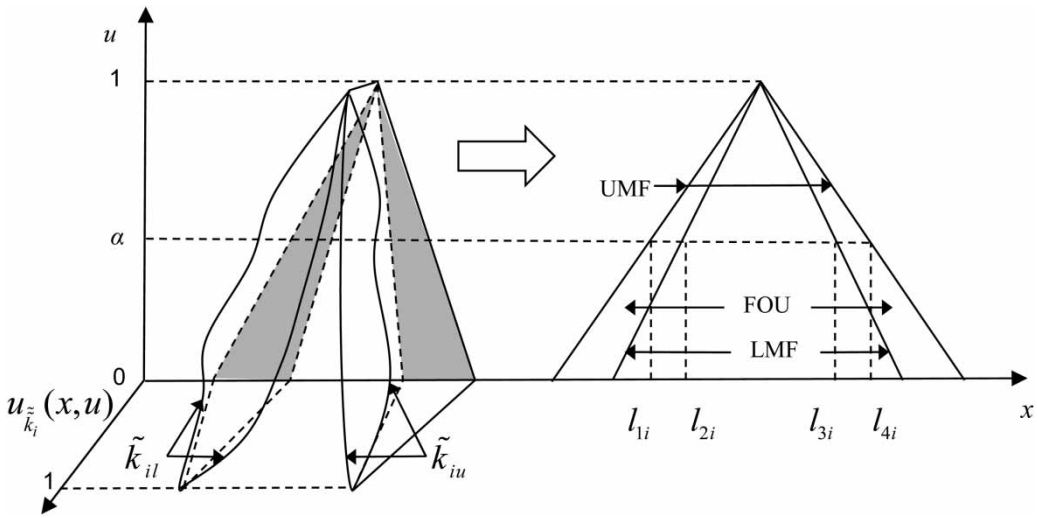

Figure 1 | T2FS.

Since T2FS can be characterized by its two membership functions, $\tilde{\tilde{A}}$ can be divided into its lover and upper bounds as follows:

$$\tilde{A}_{\alpha}^{l} = \{x \in X | \mu_{\tilde{A}^l}(x) \geq \alpha\} \tag{12}$$

$$\tilde{A}_{\alpha}^{u} = \{x \in X | \mu_{\tilde{A}^u}(x) \geq \alpha\} \tag{13}$$

For a type-2 fuzzy parameterized simulation model, each fuzzy parameter $\tilde{\tilde{k}}_i$ can be decomposed into m α-cuts leading to a set as

$$K_i = \{k_i^{(1)}, k_i^{(2)}, \ldots, k_i^{(m)}\} \tag{14}$$

where $k_i^{(j)}$ $(j = 1, 2, \ldots, m)$ represents a fuzzy dual-interval at the jth α-cut level. It can be given as

$$k_i(j) = [[\underline{k}_i^l(j), \bar{k}_i^l(j)], [\underline{k}_i^u(j), \bar{k}_i^u(j)]] \tag{15}$$

where $[\underline{k}_i^l(j), \bar{k}_i^l(j)]$ and $[\underline{k}_i^u(j), \bar{k}_i^u(j)]$ are the uncertain lower and upper bounds of parameter $\tilde{\tilde{k}}_i$ at the jth α-cut level, respectively. Obviously, when $\alpha = 1$, then $\underline{k}_i^l(1) = \bar{k}_i^l(1) = \underline{k}_i^u(1) = \bar{k}_i^u(1)$. In other words, $k_i(j)$ would converge into a single point (peak value of parameter i) with the α-cut level increasing to 1. Assume an equal distance over u axis between each pair of neighboring α-cut levels, the membership grade u_j at jth α-cut level can be given as follows:

$$u_j = \frac{(m-j)}{(m-1)}, \quad j = 1, 2, \ldots, m \tag{16}$$

The input-value vector c_i^j $(i = 1, 2, \ldots, n; j = 1, 2, \ldots, m)$ at the jth α-cut level and ith input variable can be represented as follows:

$$c_i^j = \left(\underline{k}_i^l(j), \bar{k}_i^l(j), \underline{k}_i^u(j), \bar{k}_i^u(j)\right) \tag{17}$$

TFSM method

The conventional hydrological simulation techniques typically expressed all parameters for hydrological modeling as deterministic values; however, practical hydrological simulation are complicated with a variety of uncertainties which are derived from spatial and temporal variations related to soil type, land use, slope, and agricultural management practice within the watershed (Zhang *et al.* 2014). In the SLURP model, parameters, including precipitation factor (PF) that govern the soil water movement are hard to determine precisely due to lack of monitoring data. Therefore, decision makers may mostly feel more confident in estimating the value as fuzzy sets with membership function

than giving deterministic values. In real-world cases, even the membership function may not be known with certainty; instead, they are often subjectively judged by decisions. Such information from individuals would lead to dual level fuzziness which can be expressed as T2FS. Each T2FS is defined by specifying the most credible value, the lowest and highest value of the LMF, as well as the lowest and highest value of the UMF. The most credible value (i.e. the verified parameter) is assigned a membership grade of 1, and any number that falls short of the lowest value or exceeds the highest value of the membership function would get a membership grade 0. Figure 2 illustrates the general framework of the TFSM for modeling hydrological processes. Then, Equations (5)–(8) can be formulated as follows:

$$Q_s = (\tilde{\tilde{p}} - \ln f) \cdot t \tag{18}$$

$$\mathrm{RP} + \mathrm{RI} = \frac{1}{\tilde{\tilde{k}}_1} \cdot S_1 \tag{19}$$

$$\frac{\mathrm{RP}}{\mathrm{RI}} = \frac{S_1/\tilde{\tilde{S}}_{1,\max}}{S_2/S_{2,\max}} \tag{20}$$

$$\mathrm{RG} = \frac{1}{\tilde{\tilde{k}}_2} \cdot S_2 \tag{21}$$

The calibration is conducted by both a manual method and an automatic method using the Shuffle Complex Evolution algorithm developed at the University of Arizona. Table 1 shows 10 parameters for each land type of SLURP and their assigned ranges. The goodness-of-fit of the performance of the hydrological model was assessed using the Nash–Sutcliffe efficiency (NSE), determination coefficient (R^2), and deviation of volume (DV), defined as follows:

$$\mathrm{NSE} = 1 - \frac{\sum_{i=1}^{n} (H_{\mathrm{obs},i} - H_{\mathrm{sim},i})^2}{\sum_{i=1}^{n} (H_{\mathrm{obs},i} - \bar{H}_{\mathrm{obs}})^2} \tag{22}$$

$$R^2 = \frac{\left(n \sum_{i=1}^{n} H_{\mathrm{obs},i} H_{\mathrm{sim},i} - \sum_{i=1}^{n} H_{\mathrm{obs},i} \cdot \sum_{i=1}^{n} H_{\mathrm{sim},i}\right)^2}{\left[n \sum_{i=1}^{n} H_{\mathrm{obs},i}^2 - \left(\sum_{i=1}^{n} H_{\mathrm{obs},i}\right)^2\right]\left[n \sum_{i=1}^{n} H_{\mathrm{sim},i}^2 - \left(\sum_{i=1}^{n} H_{\mathrm{sim},i}\right)^2\right]} \tag{23}$$

$$\mathrm{DV}(\%) = 100 \cdot \frac{\sum_{i=1}^{n} H_{\mathrm{obs},i} - \sum_{i=1}^{n} H_{\mathrm{sim},i}}{\sum_{i=1}^{n} H_{\mathrm{obs},i}} \tag{24}$$

where $H_{\mathrm{obs},i}$ is the observed streamflow on day i; $H_{\mathrm{sim},i}$ is the simulated streamflow on day i; n is the number of simulated days, and $\bar{H}_{\mathrm{obs}}$ is the average measured streamflow.

STUDY AREA AND DATA

The Kaidu River Basin is located in the north margin of the Yanqi Basin, Xinjinag Uygur Autonomous Region between the latitudes of 42°14′N and 43°21′N and longitudes of 82°58′E and 86°05′E (Figure 3). The catchment area of the Kaidu River above Dashankou is 18,827 km^2, with an average elevation of 3,100 m. The region has a complex topography including grassland, marsh and desert in addition to surrounding mountainous areas (Mupenzi & Li 2011). The Kaidu River Basin plays the utmost important role in protecting the Bosten Lake, the surrounding ecological environment and green corridor of the lower reaches of the Tarim River (Xu *et al.* 2013). However, massive exploitation and construction have made the regional water resources system degraded and brought about severe damage to the local ecological and environmental sustainability, such as grassland degradation, sandy desertification, and soil salinization. On the other hand, the landscape is sparsely populated, with large areas being remote and inaccessible; regular monitoring is difficulty and large investment is required; precise data are difficult to obtain due to temporal and spatial variations in hydrological processes. Data may be estimated as T2FS instead of deterministic values to gain an insight into the complicated hydrological processes. Therefore, it is deemed necessary to develop an effective approach for hydrological modeling under uncertainties to provide detailed

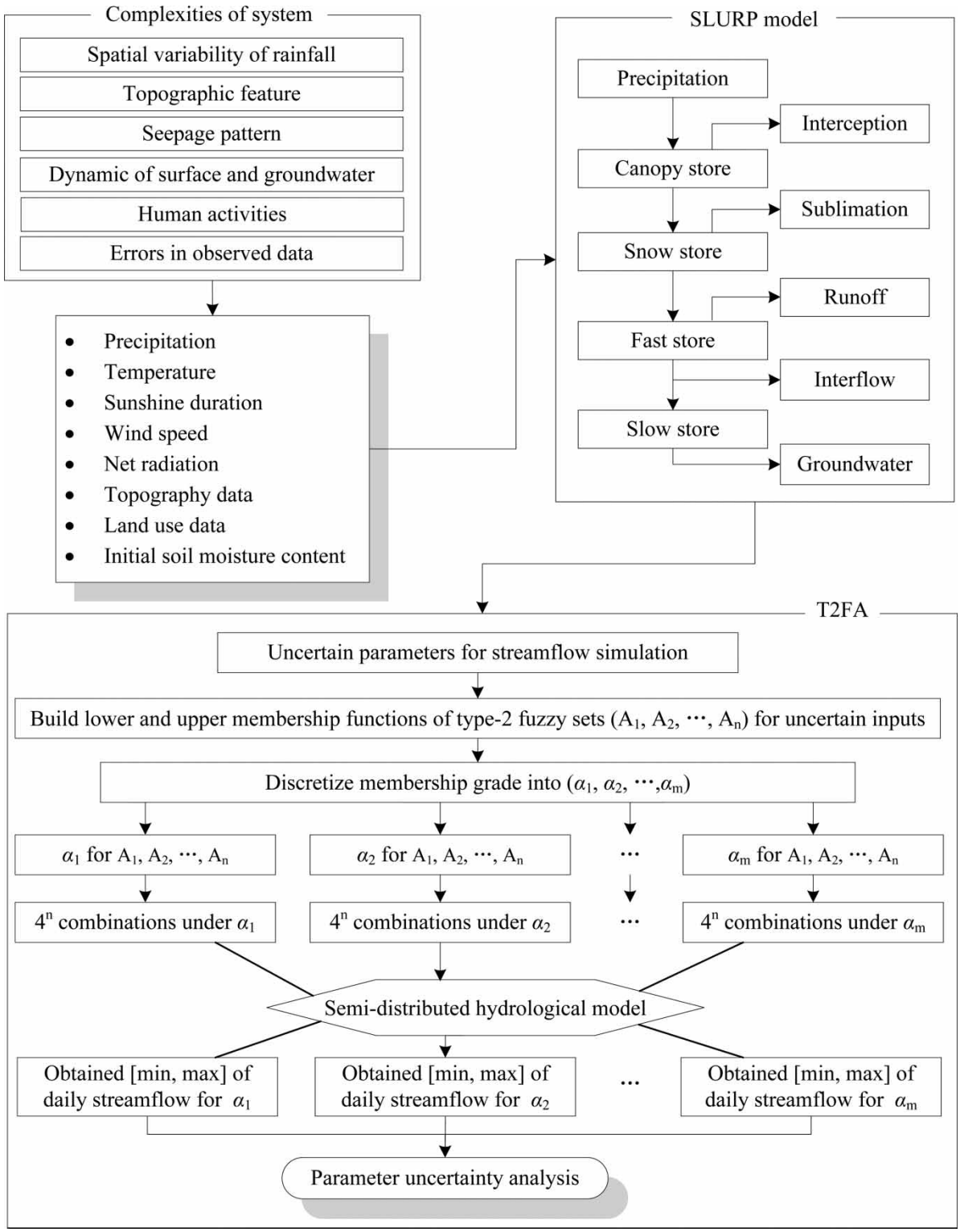

Figure 2 | General framework of the TFSM.

Table 1 | Parameters used in calibration and assigned values for the Kaidu River watershed

Parameters	Lower bound	Upper bound	Sensitivity
Initial contents of snow store (mm)	1	1,000	Low
Initial contents of slow store (%)	0	100	Low
Maximum infiltration rate (mm/d)	10	1,000	Low
Manning roughness (n)	0.0001	0.1	Low
RF (d)	1	50	High
MF (mm)	10	500	High
RS (d)	10	500	High
Maximum capacity for slow store (mm)	100	1,000	Medium
PF	0.8	15	High
Rain/snow division temperature (°C)	−2	0	Medium

information on streamflow response for water resources management (Li & Huang 2007).

The meteorological data, including air temperature, dew point temperature, precipitation, sunshine duration, wind speed, and relative humidity, are obtained from the Bayanbulak meteorological station for the period of 1996–2001. The SLURP model calculates weighted average meteorological inputs for each ASA from the monitoring data of meteorological stations using a weighted Thiessen polygon method. The temperature input for elevation differences is derived with a lapse rate of 0.75 °C per 100 m, and precipitation data are increased by 1% per 100 m based on the data obtained from the monitoring stations (Jing & Chen 2011). Daily stream flow records for the 6 years are collected from the Dashankou hydrological station, which is located at the basin outlet. The topography map is derived from the 100 × 100 m DEM. River network, ASAs characters and boundaries of watershed are obtained from the DEM using TOPAZ.

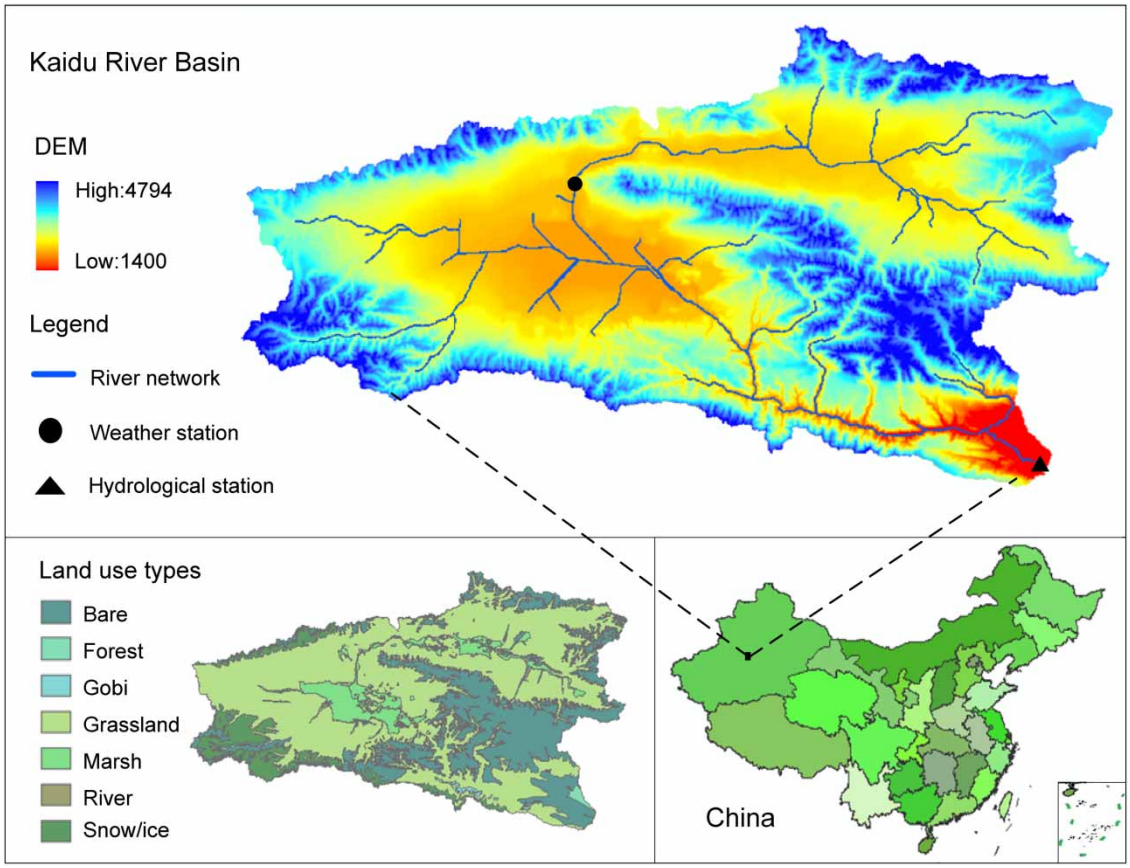

Figure 3 | Kaidu River Basin.

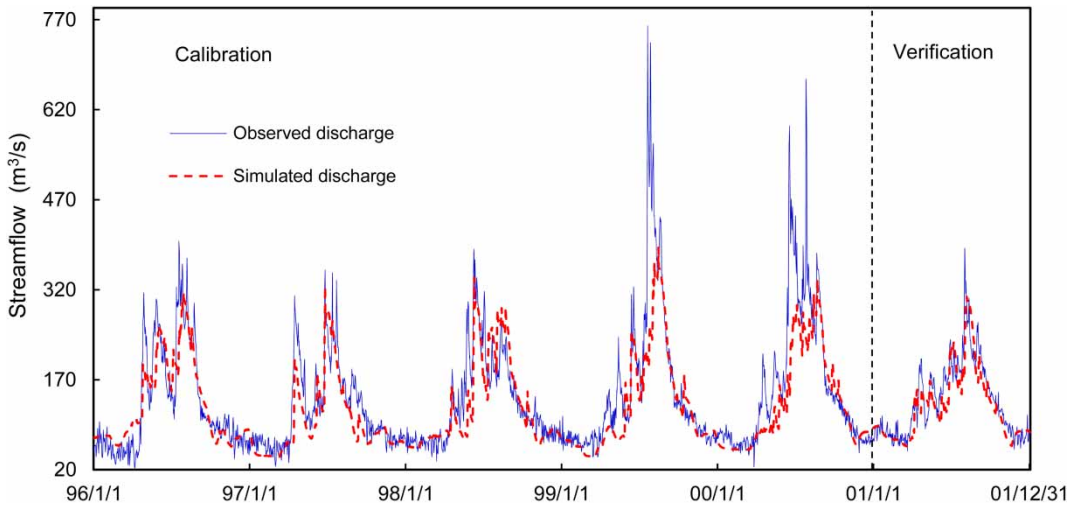

Figure 4 | Observed and simulated daily streamflow.

RESULTS AND DISCUSSION

Figure 4 illustrates the observed and simulated daily streamflow in calibration and verification periods. The NSE for calibration and verification are both above 0.6, which indicates a decent fit; the coefficients of R^2 for the two phases are both above 0.6, which indicates a good coincidence between simulated flow and the observed values. The value of DV (%) is below 10 for verification phase and slightly above 10 for calibration, indicating a low level of system error. The results also demonstrate that the simulated peak flow are underestimated during both calibration and verification periods. It might be attributed to the potential observation errors and complexities of hydrological processes. To improve the accuracy of streamflow forecasting system, four parameters, including PF, maximum capacity for fast store (MF), RF, and RS, are investigated through the type-2 fuzzy analysis technique with four α-cut levels (i.e. 0, 0.25, 0.5, and 0.75). Table 2 presents the values of the four parameters under different α-cut levels, which are expressed as dual intervals.

Table 3 presents the model performance at daily level under different α-cut levels. Since varied α-cut levels correspond to different values of the parameters, any changes in α-cut levels would yield different model performance. The values of the parameters would have significant influence on the output values of NSE, DV (%), and R^2. For example, for the parameter of RF, the value of NSE would vary from 0.49 to 0.82 under $\alpha = 0$; the interval would decrease to [0.74, 0.77] when the α-cut level increases to 0.75. The results demonstrate that the uncertainties projected in the parameters and initial conditions would significantly impact the simulated outputs; neglecting uncertainties in hydrological simulation would easily lead to a lack of information regarding system performance.

Figure 5 shows the simulated monthly peak flow and average flow under different α-cut levels. Results indicate that the fluctuation between the minimum and maximum

Table 2 | Values of fuzzy parameters under different membership grades

α-cut level	PF (–)	MF (mm)	RF (d)	RS (d)
$\alpha = 0$	[[8.0, 9.5], [13.5, 15.0]]	[[10.0, 80.0], [260.0, 330.0]]	[[1.0, 9.0], [31.0, 39.0]]	[[100, 180], [420, 500]]
$\alpha = 0.25$	[[8.8, 10.0], [13.0, 14.1]]	[[50.0, 102.5], [237.5, 290.0]]	[[5.8, 11.8], [28.3, 34.3]]	[[150, 210], [390, 450]]
$\alpha = 0.50$	[[9.8, 10.5], [12.5, 13.3]]	[[90.0, 125.0], [215.0, 250.0]]	[[10.5, 14.5], [25.5, 29.5]]	[[200, 240], [360, 400]]
$\alpha = 0.75$	[[10.6, 11.0], [12.0, 12.4]]	[[130.0,147.5], [192.5, 210.0]]	[[15.3, 17.3], [22.8, 24.8]]	[[250, 270], [330, 350]]

PF, precipitation factor; MF, maximum capacity for fast store; RF, retention constant for fast store; RS, retention constant for slow store.

Table 3 | Daily time series hydrological simulation results under different membership grades

Parameters	Values	$\alpha = 0$			$\alpha = 0.25$			$\alpha = 0.50$			$\alpha = 0.75$		
		NSE	DV (%)	R^2	NSE	DV (%)	R^2	NSE	DV (%)	R^2	NSE	DV (%)	R^2
PF	$\underline{PF}^l$	0.59	14.76	0.71	0.67	11.27	0.74	0.76	4.53	0.77	0.76	4.53	0.77
	$\overline{PF}^l$	0.71	8.89	0.75	0.74	6.47	0.76	0.76	4.74	0.77	0.76	3.52	0.77
	$\underline{PF}^u$	0.72	–6.94	0.81	0.74	–4.85	0.80	0.75	–2.96	0.80	0.76	3.52	0.77
	$\overline{PF}^u$	0.60	–12.89	0.82	0.67	–9.39	0.81	0.73	–6.14	0.81	0.76	–2.40	0.79
MF	$\underline{MF}^l$	0.49	–4.51	0.72	0.64	–6.38	0.74	0.61	1.21	0.68	0.75	0.21	0.77
	$\overline{MF}^l$	0.63	–1.00	0.70	0.63	0.80	0.68	0.75	0.31	0.77	0.74	0.49	0.77
	$\underline{MF}^u$	0.80	0.90	0.82	0.78	3.31	0.80	0.76	2.93	0.77	0.77	2.41	0.78
	$\overline{MF}^u$	0.82	–0.56	0.83	0.81	0.87	0.82	0.80	1.58	0.81	0.77	2.24	0.78
RF	$\underline{RF}^l$	0.51	–7.85	0.72	0.79	0.52	0.80	0.79	1.04	0.79	0.76	1.91	0.77
	$\overline{RF}^l$	0.76	3.03	0.77	0.80	–1.21	0.81	0.75	0.42	0.78	0.75	1.95	0.77
	$\underline{RF}^u$	0.73	0.69	0.76	0.76	0.41	0.79	0.76	1.42	0.78	0.75	0.43	0.77
	$\overline{RF}^u$	0.65	1.35	0.72	0.66	1.93	0.71	0.75	0.54	0.77	0.75	0.38	0.77
RS	$\underline{RS}^l$	0.67	–15.45	0.79	0.75	–0.18	0.76	0.68	11.85	0.77	0.68	11.40	0.77
	$\overline{RS}^l$	0.73	6.78	0.77	0.65	13.31	0.77	0.65	13.35	0.77	0.77	3.02	0.78
	$\underline{RS}^u$	0.72	2.34	0.77	0.70	8.08	0.77	0.73	7.10	0.78	0.73	5.69	0.77
	$\overline{RS}^u$	0.60	14.93	0.77	0.73	1.71	0.78	0.69	8.03	0.78	0.73	6.96	0.78

NSE, Nash–Sutcliffe efficiencies; DV, deviation of volume; R^2, determination coefficient.

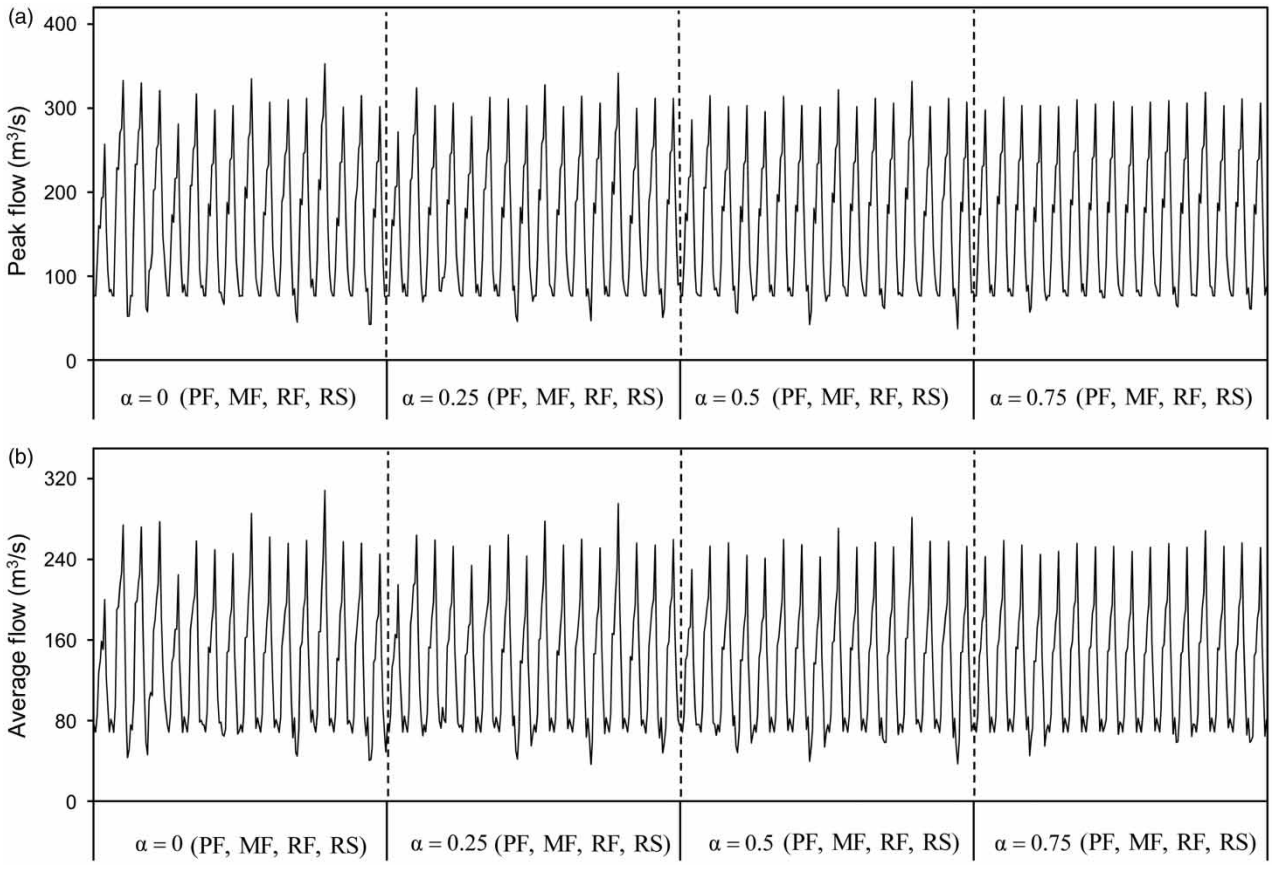

Figure 5 | Simulated monthly peak flow and average flow: (a) monthly peak flow, (b) monthly average flow.

monthly peak flow is more sensitive for PF than the other three parameters, while RF has the least effect. In detail, for PF, under $\alpha = 0.5$, the monthly peak flow would vary from 76.6 to 332 m^3/s; in comparison, the ranges of monthly peak flow would be [76.6, 315] m^3/s for MF, [76.6, 312] m^3/s for RF, [51.4, 307] m^3/s for RS. Similarly, the interval corresponding to PF would have a larger range than the other three parameters, indicating a higher uncertainty of simulation output. This is mainly because that the value of PF has significant impact on the compensation process for precipitation which directly leads to the generation of streamflow. Therefore, more attention should be paid to the value of parameter PF to enhance the prediction precision in hydrological simulation.

Figure 6 depicts the simulated daily streamflow under different parameter values. The interval between the lower and upper bounds of simulated peak flow would shrink with the α-cut level increasing. For instance, the interval of peak flow would be [288, 344] m^3/s under $\alpha = 0$; it would shrink to [292, 316] m^3/s when under $\alpha = 0.75$. The interval between the lower and upper bounds of the simulated peak flow is wider under a lower degree of plausibility (i.e. a lower α-cut level); conversely, a higher degree of plausibility would lead to a narrow interval. Figure 7 compares the simulated daily streamflow under $\alpha = 0.25$ and 0.75. The results demonstrate that different combinative considerations on the uncertain parameters would lead to varied simulation results. Thus, including the parameter uncertainty estimation as input to force the hydrological model increases the model performance, leading to more acceptable peak flow for prediction.

To identify the effects of fuzzy parameters, the simulated annual peak flow under different α-cut levels is shown in Figure 8. Different α-cut levels correspond to varied values, resulting in different simulated annual peak flow. For instance, for PF, the interval of simulated annual peak flow would be [115.1, 128.9], [128.7, 130.3], [130.3, 144.4], and [143.4, 152.5] m^3/s when the α-cut level is 0, 0.25, 0.50, 0.75. The results clearly visualize the effect of parameter uncertainties on simulated peak flow and average flow. The simulated annual peak flow and average flow would increase when the value of PF is raised. This is

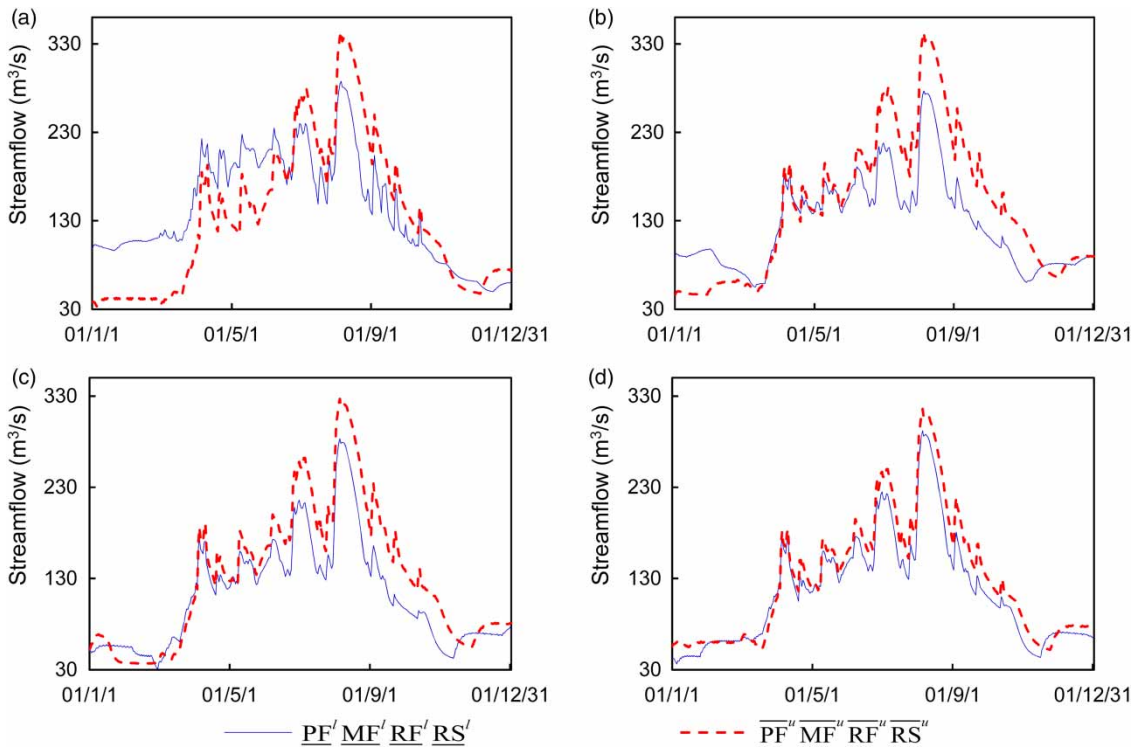

Figure 6 | Simulated daily streamflow under different parameter values: (a) $\alpha = 0$, (b) $\alpha = 0.25$, (c) $\alpha = 0.5$, (d) $\alpha = 0.75$.

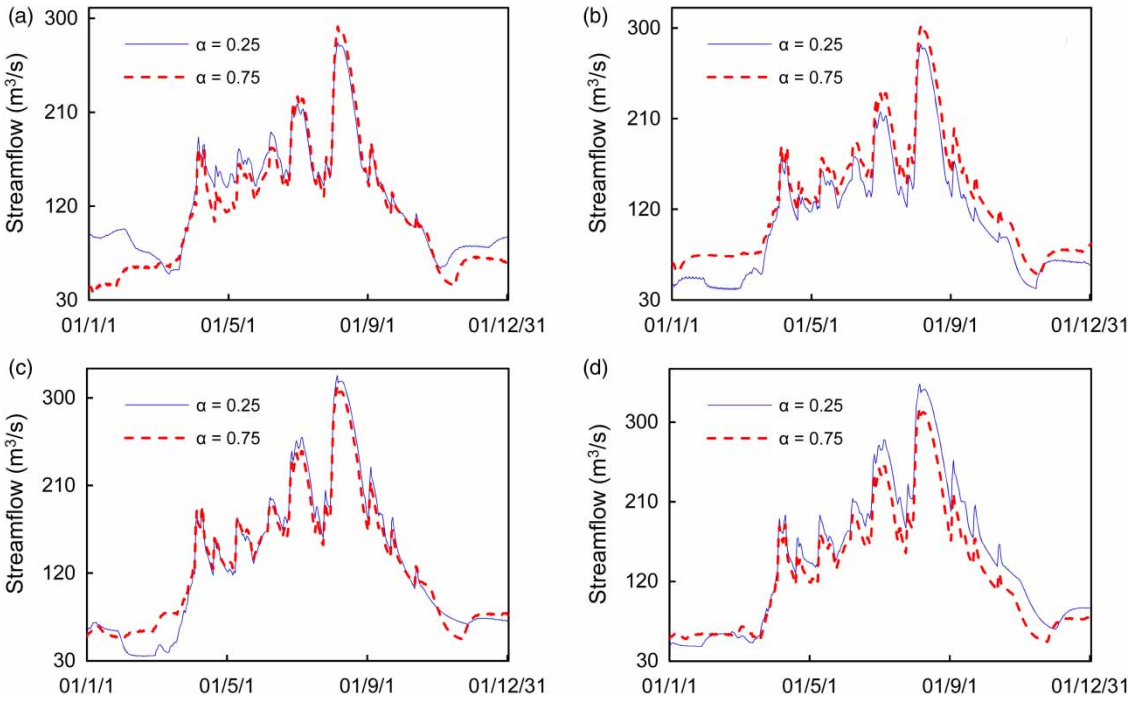

Figure 7 | Simulated daily streamflow under $\alpha = 0.25$ and 0.75: (a) $\underline{PF}^{l}\underline{MF}^{l}\underline{RF}^{l}\underline{RS}^{l}$, (b) $\overline{PF}^{l}\overline{MF}^{l}\overline{RF}^{l}\overline{RS}^{l}$, (c) $\underline{PF}^{u}\underline{MF}^{u}\underline{RF}^{u}\underline{RS}^{u}$, (d) $\overline{PF}^{u}\overline{MF}^{u}\overline{RF}^{u}\overline{RS}^{u}$.

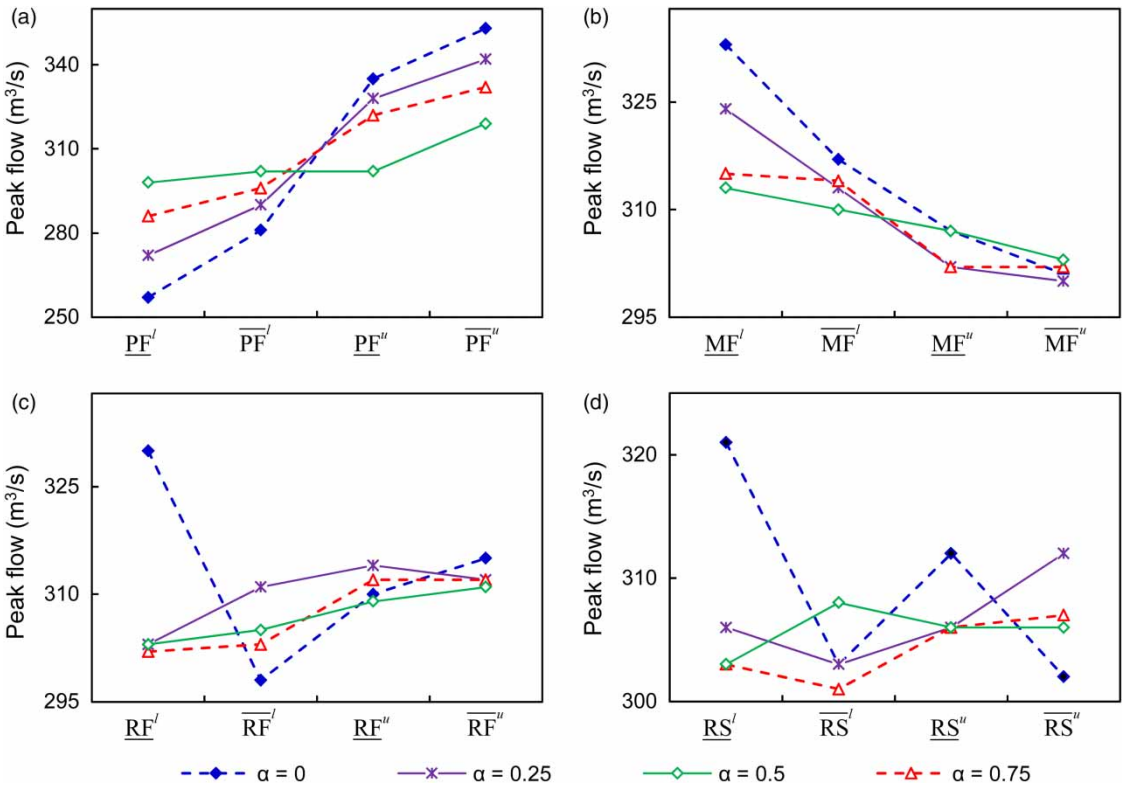

Figure 8 | Simulated annual peak flow under different α-cut levels.

because a higher PF value corresponds to a higher compensation value for the unobserved precipitation, leading to an increased streamflow associated with high level of peak flow. The simulated annual peak flow would decrease along with the MF value. This is due to the fact that MF denotes the maximum capacity of the fast store; a higher MF value is related to a highly moisture holding capacity which can lead to a low level of peak flow. Results also indicate that varied RF and RS values could also affect the peak flow; however, the variation tendency of peak flow is irregular. This is mainly because that RF related to interflow; RS related to groundwater. The two parameters indirectly affect the streamflow according to the basic equation of SLURP. Results show that estimation of streamflow in the arid region is complex due to the uncertain parameters.

CONCLUSIONS

In this study, a TFSM has been developed for assessing parameter uncertainty in the hydrological processes. Through coupling type-2 fuzzy analysis technique with the SLURP model, TFSM is useful for simulating the hydrological processes and investigating parameter uncertainties expressed as T2FS. Compared with the conventional fuzzy analysis technique which can deal with fuzzy sets with deterministic membership function, type-2 fuzzy analysis approach has advantages in handling fuzzy sets with uncertain membership function (i.e. dual uncertainties). The SLURP model is effective for dealing with spatial and temporal variations of hydrologic elements and accounts for physical mechanisms of runoff yield and routing in the watershed. The results can be used for determining the parameters of hydrological model and for reflecting parameter uncertainties in hydrological models, especially in data sparse regions.

The TFSM has also been applied to hydrological simulation for the Kaidu River Basin. The goodness-of-fit of the performance of the hydrological model has been assessed using the NSE, determination coefficient (R^2), and DV. NSE for calibration and verification are 0.65 and 0.76, respectively; R^2 for calibration and verification are 0.68 and 0.76, respectively; DV for calibration and verification are 11.37 and 7.94, respectively. The results show a good performance of SLURP in describing streamflow at the outlet of the Kaidu River Basin. Fuzzy simulation results reveal that uncertainties in PF, MF, RF, and RS have significant effects on both peak flow and average flow. Under a lower degree of plausibility (i.e. a lower α-cut level), the intervals between the lower and upper bounds of the peak flow and average flow are substantially wider whereas the interval would be narrower under a higher degree of plausibility. The results also demonstrate that the uncertainty associated with PF value has a significant effect on the simulated streamflow; in comparison, the uncertainty associated with RF has a slight effect on the simulated streamflow among the four parameters. These findings can reveal the parameter influence on hydrological simulation and improve efficiency in hydrological prediction, as well as enhance the model applicability.

The results indicate that the TFSM can effectively communicate the implicit knowledge related to the hydrological processes and reveal the effects of uncertain parameters under the assumption that the parameters are independent from each other. In many real-world problems, multiple uncertain parameters may be interrelated to each other, leading to different effects on modeling outputs. For instance, the interactive effect of two insignificant factors may be significant, or the two positive-significant factors may have a negative effect on the system response. Therefore, TFSM can be integrated with factorial analysis to reveal the potential interrelationships among a variety of uncertain parameters and their impacts on model performance. Besides, TFSM can tackle uncertainties presented as T2FS; however, many system components may be of stochastic characteristics, such as precipitation, soil properties, and slope. The PF has the feature of fuzziness and randomness, leading to hybrid uncertainties. Therefore, TFSM can be further enhanced through incorporating stochastic analysis to tackle not only parameter uncertainties presented in multiple formats, but also hybrid uncertainties expressed by fuzzy membership functions and probability distributions that exist in hydrological models. Moreover, snowmelt is one of the water resources in Kaidu River Basin; the uncertainties corresponding to snowmelt may also have an effect on the model performance. In this study, snowmelt is calculated using the degree-day considering air temperature. In fact, the process of snowmelt may also be affected by other factors such as wind speed,

shortwave and longwave radiation, vapor pressure and snow depth. Thus, TFSM may be enhanced through incorporating more effective snowmelt simulation methods into its framework to address more complex uncertainties and dynamics.

ACKNOWLEDGEMENTS

This research was supported by the National Natural Sciences Foundation (51379075, 51225904, and 51190095), the Open Research Fund Program of State Key Laboratory of Desert and Oasis Ecology, and the 111 Project (B14008). The authors are grateful to the editors and the anonymous reviewers for their insightful comments and suggestions.

REFERENCES

Ahn, S. R., Park, G. A., Jung, I. K., Lim, K. J. & Kim, S. J. 2010 Assessing hydrologic response to climate change of a stream watershed using SLURP hydrological model. *KSCE J. Civ. Eng.* **15**, 43–55.

Aishan, T., Halik, Ü., Cyffka, B., Kuba, M., Abliz, A. & Baidourela, A. 2013 Monitoring the hydrological and ecological response to water diversion in the lower reaches of the Tarim River, Northwest China. *Quatern. Int.* **311**, 155–162.

Aliev, R. A., Pedrycz, W., Guirimov, B. G., Aliev, R. R., Ilhan, U., Babagil, M. & Mammadli, S. 2011 Type-2 fuzzy neural networks with fuzzy clustering and differential evolution optimization. *Inform. Sci.* **181**, 1591–1608.

Arabi, M., Govindaraju, R. S. & Hantush, M. M. 2007 A probabilistic approach for analysis of uncertainty in the evaluation of watershed management practices. *J. Hydrol.* **333**, 459–471.

Bastola, S. & Murphy, C. 2013 Sensitivity of the performance of a conceptual rainfall-runoff model to the temporal sampling of calibration data. *Hydrol. Res.* **44**, 484–494.

Benke, K. K., Lowell, K. E. & Hamilton, A. J. 2008 Parameter uncertainty, sensitivity analysis and prediction error in a water-balance hydrological model. *Math. Comp. Model* **47**, 1134–1149.

Blasone, R. S., Vrugt, J. A., Madsen, H., Rosbjerg, D., Robinson, B. A. & Zyvoloski, G. A. 2008 Generalized likelihood uncertainty estimation (GLUE) using adaptive Markov Chain Monte Carlo sampling. *Adv. Water Resour.* **31**, 630–648.

Bourgault, M. A., Larocque, M. & Roy, M. 2014 Simulation of aquifer-peatland-river interactions under climate change. *Hydrol. Res.* **45**, 425–440.

Charles, O. & Parick, W. 2015 Uncertainty in calibrating generalised Pareto distribution to rainfall extremes in Lake Victoria basin. *Hydrol. Res.* **46** (3), 356–376. doi: 10.2166/nh.2014.052.

Guerrero, J. L., Westerberg, I. K., Halldin, S., Lundin, L. C. & Xu, C. Y. 2013 Exploring the hydrological robustness of model-parameter values with alpha shapes. *Water Resour. Res.* **49**, 6700–6715.

Han, J. C., Huang, G. H., Zhang, H., Li, Z. & Li, Y. P. 2014 Bayesian uncertainty analysis in hydrological modeling associated with watershed subdivision level: a case study of SLURP model applied to the Xiangxi River watershed, China. *Stoch. Environ. Res. Risk. Assess.* **28**, 973–989.

Huang, Y., Chen, X., Li, Y. P., Huang, G. H. & Liu, T. 2010 A fuzzy-based simulation method for modelling hydrological processes under uncertainty. *Hydrol. Process.* **24**, 3718–3732.

Hughes, D. A., Kapangaziwiri, E. & Tanner, J. 2013 Spatial scale effects on model parameter estimation and predictive uncertainty in ungauged basins. *Hydrol. Res.* **44**, 441–453.

Hughes, D. A., Mantel, S. & Mohobane, T. 2014 An assessment of the skill of downscaled GCM outputs in simulating historical patterns of rainfall variability in South Africa. *Hydrol. Res.* **45**, 134–147.

Jeremiah, E., Sisson, S. A., Sharma, A. & Marshall, L. 2012 Efficient hydrological model parameter optimization with sequential Monte Carlo sampling. *Environ. Modell. Softw.* **38**, 283–295.

Jing, L. & Chen, B. 2011 Hydrological modeling of sub-Arctic wetlands: comparison between SLURP and WATFLOOD. *Environ. Eng. Sci.* **28**, 521–533.

Kizza, M., Guerrero, J. L., Rodhe, A., Xu, C. Y. & Ntale, H. K. 2013 Modelling catchment inflows into Lake Victoria: regionalisation of the parameters of a conceptual water balance model. *Hydrol. Res.* **44**, 789–808.

Lenhart, T., Fohrer, N. & Frede, H. G. 2003 Effects of land use changes on the nutrient balance in mesoscale catchments. *Phys. Chem. Earth. Parts A/B/C* **28**, 1301–1309.

Li, Y. P. & Huang, G. H. 2007 Inexact multistage stochastic quadratic programming method for planning water resources systems under uncertainty. *Environ. Eng. Sci.* **24**, 1361–1377.

Li, Y. P. & Huang, G. H. 2009 Fuzzy-stochastic-based violation analysis method for planning water resources management systems with uncertain information. *Inform. Sci.* **179**, 4261–4276.

Li, Z. L., Shao, Q. X., Xu, Z. X. & Xu, C. Y. 2013 Uncertainty issues of a conceptual water balance model for a semi-arid watershed in north-west of China. *Hydrol. Process.* **27**, 304–312.

Ling, J., Wu, M. L., Chen, Y. F., Zhang, Y. Y. & Dong, J. D. 2014 Identification of spatial and temporal patterns of coastal waters in Sanya Bay, South China Sea by Chemometrics. *J. Environ. Inform.* **23**, 37–43.

Ma, Z. Z., Wang, Z. J., Xia, T., Gippel, C. J. & Speed, R. 2014 Hydrograph-based hydrologic alteration assessment and its application to the Yellow River. *J. Environ. Inform.* **23**, 1–13.

Mahiny, A. S. & Clarke, K. C. 2013 Simulating hydrologic impacts of urban growth using SLEUTH, multi criteria evaluation and runoff modeling. *J. Environ. Inform.* **22**, 27–38.

Muleta, M. K. & Nicklow, J. W. 2005 Sensitivity and uncertainty analysis coupled with automatic calibration for a distributed watershed model. *J. Hydrol.* **306**, 127–145.

Mupenzi, J. P. & Li, L. 2011 Impacts of global warming perturbation on water resources in arid zone: case study of Kaidu River Basin in Northwest China. *J. Mountain Sci.* **8**, 704–710.

O'Loughlin, F., Bruen, M. & Wagener, T. 2013 Parameter sensitivity of a watershed-scale flood forecasting model as a function of modelling time-step. *Hydrol. Res.* **44**, 334–350.

Patel, H. & Rahman, A. 2015 Probabilistic nature of storage delay parameter of the hydrologic model RORB: a case study for the Cooper's Creek catchment in Australia. *Hydrol. Res.* **46** (3), 400–410. doi: 10.2166/nh.2014.172.

Shiri, J., Marti, P., Nazemi, A. H., Sadraddini, A. A., Kisi, O., Landeras, G. & Fard, A. F. 2015 Local vs. external training of neuro-fuzzy and neural networks models for estimating reference evapotranspiration assessed through k-fold testing. *Hydrol. Res.* **46** (1), 72–88.

Vincendon, B., Ducrocq, V., Saulnier, G. M., Bouilloud, L., Chancibault, K., Habets, F. & Noilhan, J. 2010 Benefit of coupling the ISBA land surface model with a TOPMODEL hydrological model version dedicated to Mediterranean flash-floods. *J. Hydrol.* **394**, 256–266.

Wang, L. Z., Huang, Y. F., Wang, L. & Wang, G. Q. 2014 Pollutant flushing characterizations of stormwater runoff and their correlation with land use in a rapidly urbanizing watershed. *J. Environ. Inform.* **23**, 44–54.

Westerberg, I. K., Gong, L., Beven, K. J., Seibert, J., Semedo, A., Xu, C. Y. & Halldin, S. 2014 Regional water balance modelling using flow-duration curves with observational uncertainties. *Hydrol. Earth Syst. Sci.* **18**, 2993–3013.

Xu, J. H., Chen, Y. N., Li, W. H., Peng, P. Y., Yang, Y., Song, C. N., Wei, C. M. & Hong, Y. L. 2013 Combining BPANN and wavelet analysis to simulate hydro-climatic processes – a case study of the Kaidu River, North-west China. *Front. Earth Sci.* **7**, 227–237.

Zhang, X., Srinivasan, R. & Bosch, D. 2009 Calibration and uncertainty analysis of the SWAT model using genetic algorithms and Bayesian model averaging. *J. Hydrol.* **374**, 307–317.

Zhang, J. L., Li, Y. P. & Huang, G. H. 2014 A robust simulation-optimization modeling system for effluent trading – a case study of nonpoint source pollution control. *Environ. Sci. Pollut. Res. Int.* **21**, 5036–5053.

Zhou, F., Xu, Y. P., Chen, Y., Xu, C. Y., Gao, Y. Q. & Du, J. K. 2013 Hydrological response to urbanization at different spatio-temporal scales simulated by coupling of CLUE-S and the SWAT model in the Yangtze River Delta region. *J. Hydrol.* **485**, 113–125.

First received 18 December 2014; accepted in revised form 5 February 2015. Available online 9 March 2015